Journal of the European Ceramic Society 17 (1997) 1855–1860

PII: S0955-2219(97)00067-8
0955-2219/97/$17.00 + 0.00

Cyclic Fatigue Behaviour of Silicon Nitride Materials

J. Bermudo,[a] M. I. Osendi,[a] M. Li[b] and M. J. Reece[b]

[a]Instituto de Ceramica y Vidrio, CSIC, 28500 Arganda del Rey, Madrid, Spain
[b]Queen Mary and Westfield College, University of London, London, UK

Abstract

The cyclic fatigue behaviour of two silicon nitride materials have been investigated. Both ceramics were prepared under the same processing conditions from two different types of silicon nitride powders. One of the powders was obtained by self-propagation high temperature synthesis (SHS), and the other by a commercial route. Materials have been fully characterized using conventional techniques of XRD and SEM. Fatigue tests on double cantilever beam-type specimens, at a frequency of 10 Hz and a load rate of $R = 0{\cdot}125$, have been performed under tension–tension cyclic fatigue, and under tensile static fatigue. Crack growth was measured with a travelling microscope focused on the specimen surface. Crack growth parameters were obtained assuming a Paris power law dependence. The results obtained from these analyses and the study of fracture surfaces on both materials have been correlated to the fatigue mechanism. © *1997 Elsevier Science Limited.*

1 Introduction

Silicon nitride is one of the most interesting materials for structural applications due to its excellent strength retention at high temperatures, adequate toughness and good thermal shock resistance. An important characterisitic of silicon nitride ceramics is the 'in situ reinforcement mechanism' produced by their microstructure.[1] This toughening mechanism is due to bridging and pull-out phenomena induced by the whisker-like β-Si_3N_4 grains developed in the ceramic during the sintering process.

In recent years, the cyclic fatigue behaviour of silicon nitride has been actively investigated[2,3] because mechanical degradation under cyclic load conditions is relevant to the engineering applications of silicon nitride.[4,5] The fatigue in Si_3N_4 has been attributed to microstructural damage produced by the cyclic nature of the stress.[6–10] In the present work, static and cyclic fatigue behaviour at room temperature have been studied on two different silicon nitride powders densified by hot-pressing techniques. One of the silicon nitride powders was obtained by self-propagating high-temperature synthesis (SHS), and the other was from a commercial source, prepared by the traditional production/synthesis route. The aim of the present work was to compare the fatigue behaviour of both materials.

2 Experimental Techniques

2.1 Specimen design and fabrication

An experimental silicon nitride powder batch obtained using SHS reactions by SHS-España (Paracuellos, Spain) and silicon nitride powder (LC 12) commercialized by H. C. Starck (Germany) were used as the starting raw materials. The physical parameters of the powders are shown in Table 1.

Both powders were mixed with the oxide additive (10 mass % Y_2O_3) in an attrition mill for 1 h. Each powder mixture was hot-pressed at 1750°C/90 min and 50 MPa of pressure in a nitrogen atmosphere (0·1 MPa), and disks of 50-mm diameter were obtained. The density, calculated by Archimedes' method, and Young's modulus of the materials, measured by ultrasonic techniques, are given in Table 2. α-Si_3N_4 and $Y_{4{\cdot}67}\ O_{13}\ Si_3$ as secondary phase were identified in the two materials. Samples of both materials were polished and plasma-etched to show the microstructure obtained after the sintering process. The grain structure was bimodal and similar in scale for both materials (Figs 1 and 2). The grain size of the equiaxed grains was typically 1 μm. The aspect ratio of the whisker-like grains was approximately 4.

Table 1. Characteristics of the silicon nitride powders

Powders	d_{50} (μm)	S_{BET} (m^2gr^{-1})	O_2 (%mass)
LC12 (Starck)	0·8	22	1·9
SHS*	0·4	11·7	2·4

*Powder attrition milled with Si_3N_4 balls.

Table 2. Densities and Young's Modulus in both nitrides

Material	*Density (g cc^{-1})*	*Young's Modulus (GPa)*
HP–Starck	3·26	330
HP–SHS	3·22	326

The hot-pressed disks were machined to obtain double cantilever beam-type specimens with the geometry shown in Fig. 3. A notch (10–11 mm long) was introduced in all the specimens. The HP–SHS specimen was precracked by forcing a wedge into the notch. The HP–Starck specimen was cracked by fatigue loading.

2.2 Experimental procedure

Specimens were attached to the fixtures using metal pins, which were held in position with epoxy resin while a small tensile load was applied. The notch opening displacement was measured using a capacitance transducer with a resolution of 0·2 ptm mV^{-1}, attached at the back of the specimens. It enabled load versus notch opening displacement curves to be plotted during the tests. The crack growth was measured with a travelling microscope with a resolution of 10 μm.

The cyclic loading was carried out in a servohydraulic machine at room temperature at 50 ± 10% relative humidity. The load ratio R ($R = P_{min}/P_{max}$) was 0·125 and the frequency was 10 Hz. The static fatigue tests were performed on each specimens after the cracks had grown 7–8 mm during the cyclic fatigue tests.

The applied stress intensity factor (K) was determined from the Wilson-Newman expression.[11]

$$\frac{KBw^{1/2}}{P} = \frac{2 + a/w}{(1 - a/w)^{3/2}} \times [0{\cdot}8072 + 8{\cdot}858(a/w) - 30{\cdot}32(a/w)^2 + 41{\cdot}088(a/w)^3 - 24{\cdot}15(a/w)^4 + 4{\cdot}915(a/w)^5]$$

where P is the applied load, B is the specimen thickness, W is the width of the specimen and a is the crack length from the centre of the load line to the crack tip. The Wilson-Newman expression is valid in the range $0{\cdot}2 < a/w < 1$.[11] The accuracy of fit is better than 0·5%.

3 Experimental Results and Discussion

The results of the fatigue tests on both materials are shown in Figs 4 and 5, where the normalized crack length is plotted as a function of time for the different cyclic and static loading conditions. At the beginning of test the precrack (a/w = 0·095) in the HP–SHS specimen had a different length on each side of the specimen; they eventually became equal after growing a few millimeters (a/w = 0·147) during cyclic loading. The initial normalized notch length in the HP–Starck specimen was 0·104. Figures 4 and 5 also show the value of the maximum applied load used during the testing. The load amplitudes were chosen so as to obtain stable

Fig. 1. Microstructure of the HP–SHS material hot-pressed.

Fig. 2. Microstructure of the HP–Starck material hot-pressed.

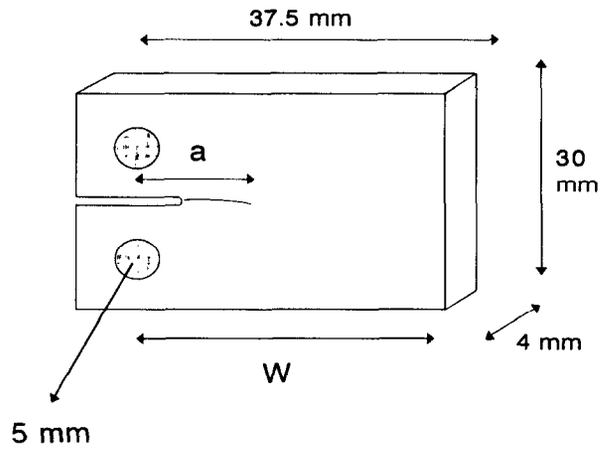

Fig. 3. Geometry of the test specimens.

crack growth rates and they were reduced when the cracks began to grow too fast ($> 10^{-6}$ m sec^{-1}) to be measured accurately. The maximum cyclic load had to be increased to +700N to initiate a crack in the HP–Starck material. The precrack in the HP–SHS material required a similar maximum cyclic load to cause it to propagate.

Plots of crack growth rates (da/dt) versus maximum applied stress intensity factor (K_{max}) are shown in Figs 6 and 7 for both silicon nitride materials. The V-K data do show a small dependence on crack length, something that has also been reported for other materials.[12] To distinguish this difference, the cyclic data have been plotted in two data sets, zones A and B corresponding to relatively short and long crack lengths, respectively. In the HP–SHS material, the zone A represents a/w values between 0·21 and 0·25 and, in the HP–Starck material, it represents crack lengths between 0·21 and 0·26. The zone B in the HP–SHS has a/w values between 0·26 and 0·31, and in the HP–Starck, the values of a/w are 0·27 and 0·34.

Linear fits for the log–log plots of the V-K data yielded values for the exponent in the Paris power law relation $da/dt = A(K_{max})^n$. For the HP–SHS material the n values are 31 and 27 for the cyclic fatigue data sets and 142 for the static data (Fig. 6). For the HP–Starck material, the n values are 30 and 27 for the cyclic data sets and 101 for the static data (Fig. 7). The results for both materials are similar within the uncertainty of the measurement. Figures 6 and 7 show different threshold values of K_{max} for crack growth under cyclic and static loadings. For both the HP–Starck and HP–SHS materials, the crack stopped propagating when K_{max} was lower than 4·6 MPam$^{1/2}$ and 6·2 MPam$^{1/2}$ for cyclic and static loading, respectively. The higher values of K_{max} required in static fatigue to achieve the same growth rate as in cyclic fatigue and the larger stress exponents for static fatigue compared to cyclic fatigue is common for a number of ceramic materials.[13]

The evolution of load versus the notch opening–displacement curves as a function of increasing length are illustrated in the plots of Figs 8 and 9. No hysteresis loops were observed in any of the materials under study, even for the longest crack lengths. The fatigue cracks can be characterised using the analysis of crack hysteresis curves developed by Guiu *et al.* and originally applied to alumina materials.[14] Figures 10 and 11 show 'relaxed compliance' compared with 'calibrated compliance' at each crack length. The 'relaxed compliance' was measured from the slope of the tensile part of the

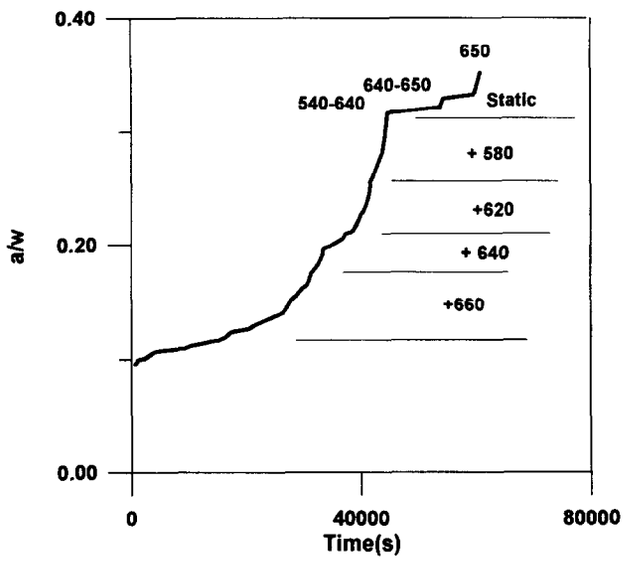

Fig. 4. Normalized crack-length (a/w) versus cycles for the HP–SHS material. Numbers with + sign indicate tension–tension cycling loading and numbers without sign + indicate static loading.

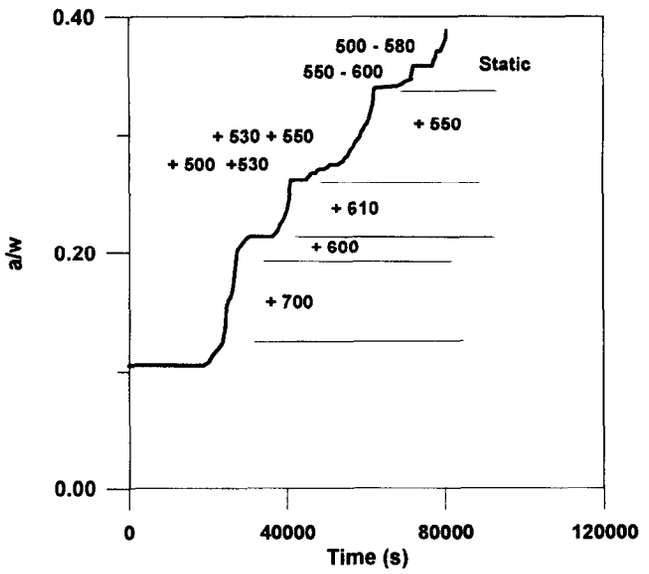

Fig. 5. Normalized crack-length (a/w) versus cycles for the HP–Starck material. Numbers with + sign indicate tension–tension cycling loading and numbers without sign + indicate static loading.

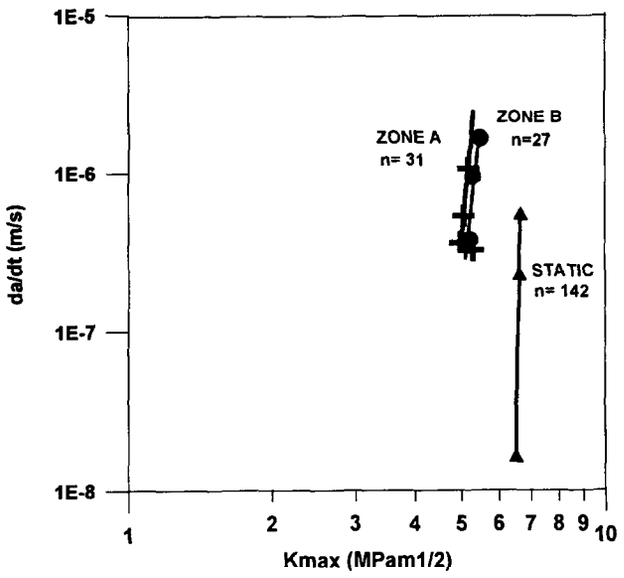

Fig. 6. Crack growth rate (da/dt) versus K_{max} applied in HP–SHS material.

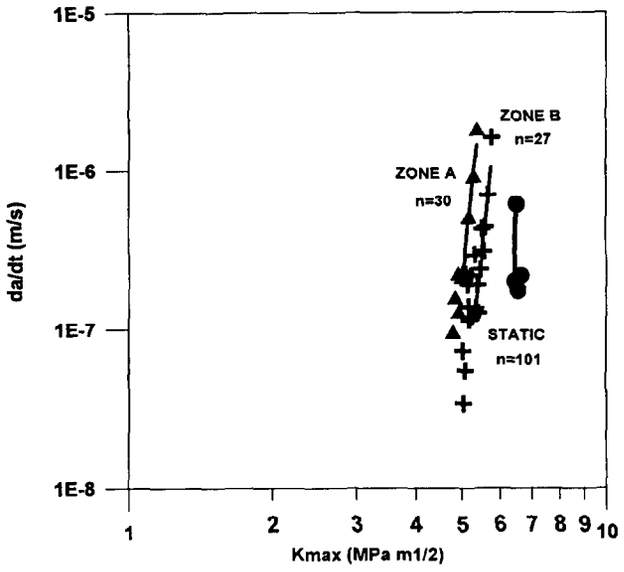

Fig. 7. Crack growth rate (da/dt) versus K_{max} applied in HP–Starck material.

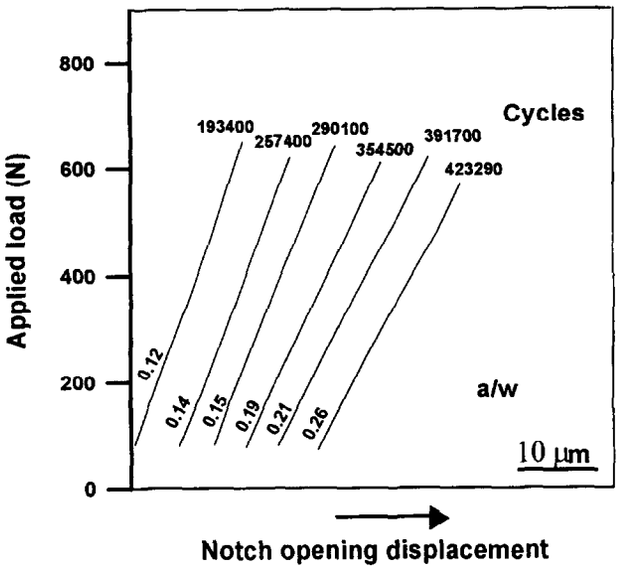

Fig. 8. Load–crack opening displacement curves from the HP–SHS material.

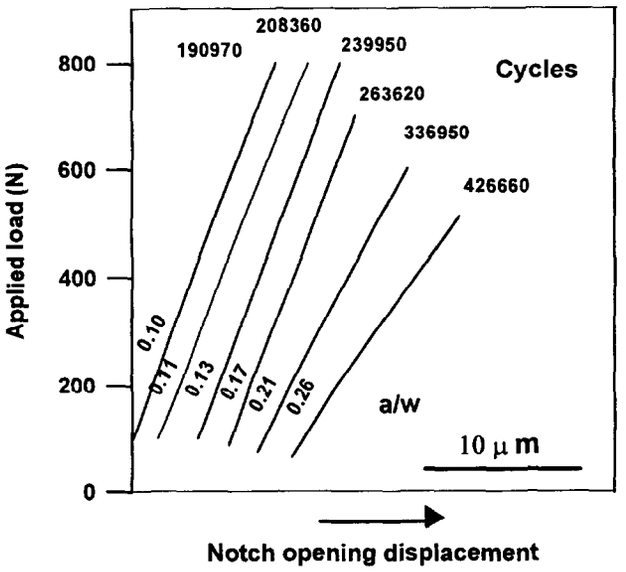

Fig. 9. Load–crack opening displacement curves from the HP–Starck material.

load– displacement curves. The 'calibrated compliance' was obtained experimentally using a specimen into which notches or variable length were cut. Therefore, the calibrated data is not influenced by the effect of bridging ligaments or any other crack closure effects. The results clearly show that the relaxed compliance is always smaller than the calibrated compliance for the same crack length. This indicates that the fatigue cracks in silicon nitride are restrained by closure forces probably produced by crack bridging ligaments in the crack wake.

The applied load, P_A is the sum of three components, $P_A = P_e + P_f + P$[14]. P_e is the total load carried by the elastic bridging ligaments; P_f is the total frictional force of the sliding ligaments (given by half the vertical width of hysteresis loop); and P is the load needed to produce the same crack opening displacement in an unbridged free crack. For the silicon nitride materials in this study, $P_f = 0$, as indicated by the absence of hysteresis loops in Figs 8 and 9. P_e can be calculated from the relaxed and calibrated compliance for each crack length. Figures 12 and 13 show the normalized elastic bridging load, P_e, with respect to the total applied load, P_{max}, against the crack length. The contribution of P_e increased with increasing crack length as the number of bridging ligaments initially increased. Eventually, the effective bridging length saturated and the elastic contribution plateaued at 30% of the applied load. Similar magnitudes for the normalised elastic bridging contribution to crack shielding have been reported for silicon nitride[15] and alumina.[14–16]

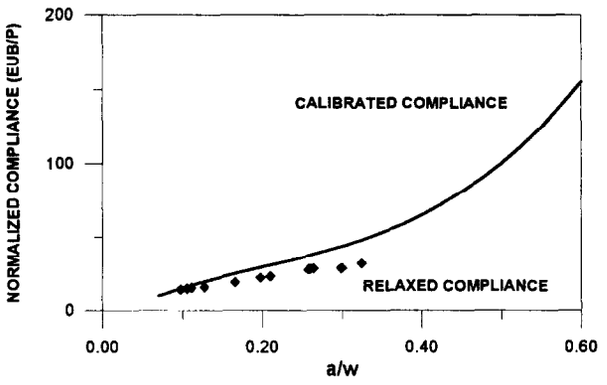

Fig. 10. EUB/P versus crack length results for the HP–Starck material.

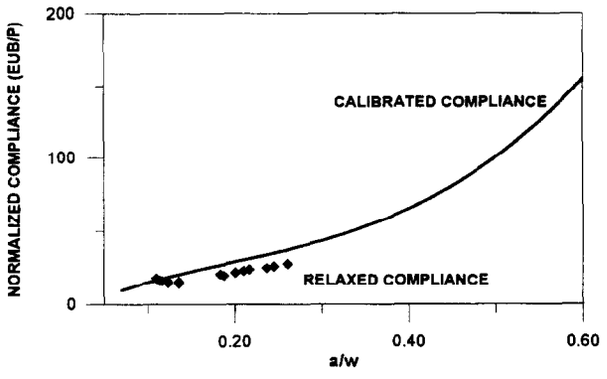

Fig. 11. EUB/P versus crack length results for the HP–SHS material.

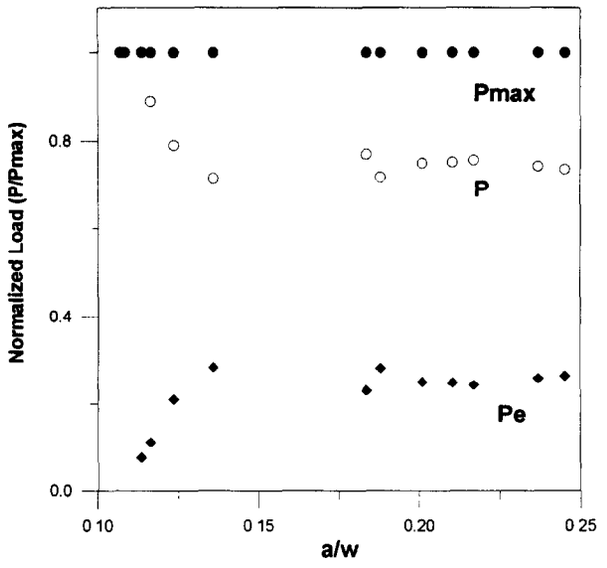

Fig. 12. Evolution of the different components of the load with a/w in the HP–SHS material.

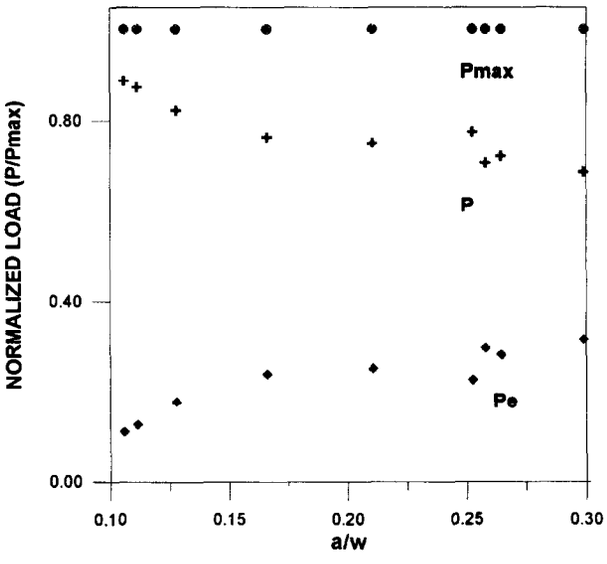

Fig. 13. Evolution of the different components of the load with a/w in the HP–Starck material.

The degradation of the elastic and frictional bridging ligaments is a potential mechanism for cyclic fatigue damage in ceramics. The reduction of the closure forces that this produces increases the K experienced by the crack tip, causing a crack growth increment. This is accompanied by the development of a new bridged section of crack wake at the crack tip. This continual development of the bridged crack wake stabilizes the crack giving rise to fatigue crack growth. Therefore, the effect of cyclic fatigue is only observed in materials that have an intergranular crack path which can produce geometric bridging ligaments. Horibe and Hirahara showed that, in sintered silicon nitride which was produced without additives, fatigue cracks propagated transgranularly and no true cyclic fatigue effect was observed.[17] When silicon nitride was sintered with additives, the crack path propagated intergranularly and cyclic fatigue effects were observed. Microstructural observation of fracture surfaces on the silicon nitride materials (Figs 14 and 15) show the intergranular fracture and the pull out of β-Si_3N_4 grains.

The frictional contribution to the crack shielding in the silicon nitride materials is relatively small, as is evidenced by the narrow hysteresis loops. In alumina materials, including fine grain size alumina ($4\,\mu m$)[14] and some silicon nitrides,[18] a measurable frictional component has been detected. In all cases, the frictional component was significantly smaller than the elastic component. Considering the intergranular fracture surface of our materials and the observation of the pull out of elongated grains, the lack of a measurable frictional component is surprising. One possible explanation for this is that the effective bridging ligaments that shield the crack tip are highly constrained and are close to the crack tip. They would then produce large closure forces without necessarily producing a significant frictional effect. The mechanism of fatigue would then require the fracture of these ligaments under the closure forces during cyclic loading.

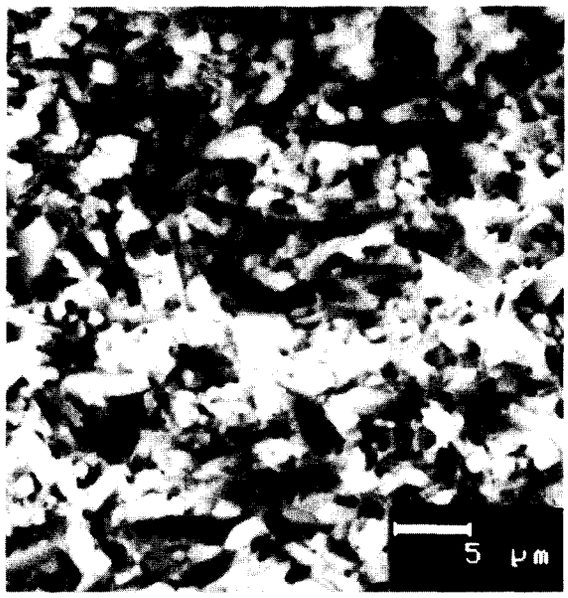

Fig. 14. Cyclic fracture surface of the HP–SHS.

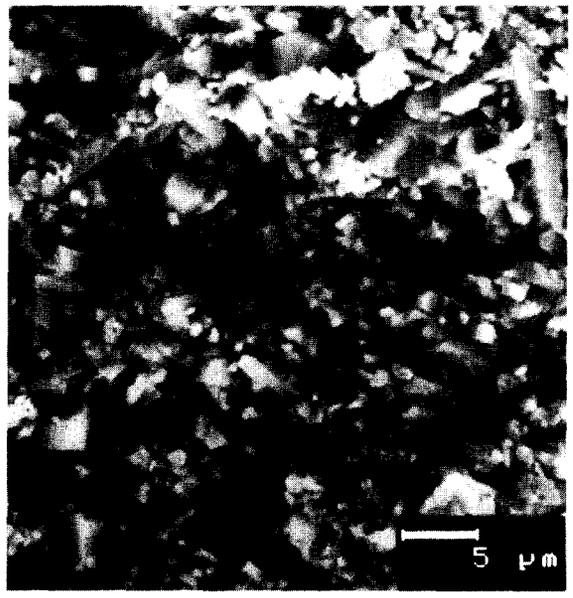

Fig. 15. Cyclic fracture surface of the HP–Starck.

4 Conclusions

The following general conclusions can be drawn:

1. The elastic bridging was the main crack shielding process in the silicon nitride materials studied (30% of the applied load).
2. The bridging area remained constant during the cyclic fatigue test, after the crack had grown a short distance (25 μm).
3. Both silicon nitrides degraded faster under cyclic loading than under static loading conditions.
4. The fatigue behaviour in both silicon nitride materials followed a Paris law expression.
5. Their fatigue behaviour was quite similar.

Acknowledgements

We would like to thank the economical support to 'PROMETHEUS Project', Spain, MAT95-1239-E, Spain and The Royal Society grant 626006.F601/LM, UK. We would like to thank, as well, the British Council and the C.SI.C. for their Support under the 'Acciones Integradas' programme.

References

1. Kishimoto, H., Ueno, A. and Kawamoto, H., In *Mechanical behavior of materials (VI)*, Vol. 2, ed. by M. Jono and T. Inove. Pergamon Press, Oxford, 1991, p. 375.
2. Okazaki, M., McEvily, A. J. and Tanaka, T., On the mechanism of fatigue crack growth in silicon nitride. *Met. Trans. A*, 1991, **22**, 1425.
3. Okazaki, M., McEvily, A. J. and Tanaka, T., The wedge mechanism of fatigue crack growth in silicon nitride. *Materials Science and Engineering A*, 1991, **143**, 135–141.
4. Jacobs, D. S. and Chen, I. W., Cyclic Fatigue in ceramics: a balance between crack shielding accumulation and degradation. *Journal Am. Ceram. Soc.*, 1995, **78**(3), 513–520.
5. Horibe, S., Fatigue of silicon nitride ceramics under cycling loadings. *Journal Europ. Ceram. Soc.*, 1990, **6**, 89–95.
6. Oda, I., Matsui, M., Soma, T. and Masuda, M., Fatigue of ceramics (Part 1). *Journal Ceram. Soc. Jap. Int. Ed*, 1988, **96**, 275–280.
7. Nikkilä, A. P. and Mäntila, T. A., Cyclic fatigue of silicon nitrides. 13th Annual Conference on Composites and Advanced Ceramics. Cocoa Beach, FL, October 1989, 15–18.
8. Kawakubo, T. and Komeya, K., Static and cyclic fatigue behavior of sintered silicon nitride at room temperature. *Journal Am. Ceram. Soc.*, 1987, **70**, 400–405.
9. Grathwöhl, G., *Mat.-Wiss. u. Werkstofftech*, 1988, **19**, 113. Cyclic Fatigue in Ceramics, ed. H. Kishimoto, T., Koshide and N. Okabe. Current Japanese Materials Research, 1995, V(14).
10. Tajima, Y., Urashimaa, K., Watanabe, M. and Matsuo, Y. Static, cyclic, and dynamic fatigue behaviour of silicon nitride. Proc. of the Int. Symp. on Ceram. Mat & Comp for Eng., ed. V. J. Tennery. Las Vegas, Nevada, 27–30 November 1988, 719–728.
11. Saxena, A. and Hudak Jr., S. J., Review and extension of compliance information for common crack growth specimens. *Int. Journal of Fracture*, 1978, **14**, 453–468.
12. Choi, G. and Horibe, S., R-curve and fatigue crack growth behaviour in silicon nitride ceramics. *Journal of the Ceramic Society of Japan, Int. edit.*, 1995, **103**, 685.
13. Jacobs, D. S. and Chen, I. W., Mechanical and environmental factors in the cyclic and static fatigue of silicon nitride ceramics. *Journal Am. Ceram. Soc.*, 1994, **77**(5), 1153–1561.
14. Guiu, F., Li, M. and Reece, M. J., Role of crack-bridging ligaments in the cyclic fatigue behavior of alumina. *Journal Am. Ceram. Soc.*, 1992, **75**(11), 2976–2984.
15. Urashima, K., Tajima, Y. and Watanave, M., Cyclic fatigue behavior of in-situ toughened silicon nitrides'. In *Cyclic Fatigue in Ceramics*, ed. H. Kishimoto, T. Hoshide and N. Okabe. The Society of Materials Science Japan, Elsevier Science, 1995, pp. 83–100.
16. Bartolomé, J. F., Requena, J., Moya, J. S., Li, M. and Guiu, F., Cyclic fatigue crack growth resistance of Al_2O_3–Al_2TiO_5. *Acta Mater.*, 1996, **44**(4), 1361–1370.
17. Horibe, S. and Hirahara, R., Cyclic fatigue of ceramic materials: influence of crack path and fatigue mechanism. *Acta. Metall. Mater.*, 1991, **39**(6), 1309–1317.
18. Gilbert, C., Reinhold, J., Dauskardt, H. and Ritchie, R. O., Behavior of cyclic fatigue in monolithic silicon nitride. *Journal Am. Ceram. Soc.*, 1995, **78**(9), 2291–2300.